PACS 81.40.Ef

The effect of annealing within a thermal stability interval on peculiar properties of structure formed in steel Fe-Mo-V-Nb-0.08C by high-pressure torsion

E. Astafurova[1,†], G. Maier[1], V. Koshovkina[2], E. Melnikov[1], E. Naydenkin[1], A. Smirnov[3], V. Bataev[3], P. Odessky[4], S. Dobatkin[5]

[†]elena.g.astafurova@gmail.com

[1]Institute of Strength Physics and Materials Science, 2/4, Akademicheskiy av., 634055, Tomsk, Russia
[2]National Research Tomsk Polytechnic University, 30, Lenina av., 634050, Tomsk, Russia
[3]Novosibirsk State Technical University, 20, Karla Marxa str., 630073, Novosibirsk, Russia
[4]Kucherenko Central Scientific-Research Institute of Engineering Constructions, 6, the 2nd Institutskaya str., 109428, Moscow, Russia
[5]Baikov Institute of Metallurgy and Material Science RAS, 49, Leninskiy av., 119991, Moscow, Russia

We studied the effect of annealing in the range of thermal stability on a structure produced by cold high-pressure torsion (at room temperature) in Fe-Mo-V-Nb microalloyed steel. Plastic deformation of the steel leads to the formation of a mixed submicrocrystalline structure with the size of the elements of *d*=100 nm, which are bounded with high-angle boundaries and subboundaries and contain a high dislocation density. Submicrocrystalline structure is stabilized by dispersed cementite particles M_3C (15 – 20 nm) and ultrafine (<5 nm) phases MC (M = V, Nb, Ti) and M_3C. After one-hour annealing at 500°C, the average size of the structural elements (microcrystallites) increases to d = 112 nm, and the character of their size distribution changes slightly compared with the state after high-pressure torsion. Microhardness of the steel increases from 6.0 GPa in state after high-pressure torsion up to 6.4 GPa after annealing at 500°C. During the annealing of the steel, a partial relaxation of the severely deformed structure and boundaries occurs, as well as the formation of thermally activated nuclei of recrystallization. The sizes of these nuclei are close to the values for the crystallites and the subgrains produced by high-pressure torsion. Indexing and analysis of microdiffraction patterns suggest an additional formation of nanoscale cementite particles during annealing at 500 °C. Precipitation hardening (the formation of nano-sized particles) and an increase in the fraction of high-angle boundaries due to the formation of recrystallization nuclei are responsible for the increase in microhardness value and the preservation of submicrocrystalline character of steel structure after annealing at 500°C.

Keywords: steel, submicrocrystalline structure, thermal stability, annealing, dispersion hardening.

1. Introduction

Modern trends in material science are aimed to construct the high-strength materials with simultaneous specific gravity decrease. With this regard the creation of ultrafine-grained (submicrocrystalline, nanocrystalline and nanostructural) conditions by severe plastic deformation in structural steels have good perspectives for development and industrial application providing the solution of all the basic tasks arising during these materials formation — increase of obtained raw parts scale, their uniformity and structure stability to different internal impact.

Ultrafine-grained metal materials formed by severe plastic deformation are characterized by small size of structure elements, high volume fraction of interfaces and a high level of nonequilibrium [1 – 2]. It resulted in decrease of thermal stability of these materials if compare with coarse-grained analogues [1 – 2].

Stabilization of ultrafine-grained steels structure is successfully obtained by refractory elements alloying which forms dispersed particles resistant to annealing and deformation. Thus, it makes it possible to increase the strength properties and recrystallization start temperature in microalloyed steels with ultrafine-grained structure in comparison with, for example, ultrafine-grained armco-iron or low carbon steels [3 – 5].

This work is aimed to find out the peculiar properties of grain-subgrain structure, phase composition and carbide subsystem in Fe-Mo-V-Nb steel processed by high-pressure torsion and annealed within an interval of thermal stability of ultrafine-grained (submicrocrystalline) state (at 500°C).

2. Research methods

Fire-resistant steel Fe-Mo-V-Nb (Fe-0.08Mo-0.63Mn-0.75Cr-0.18Ni-0.38Si-0.17Cu-0.03Ti-0.05V-0.03Nb- 0.08C, wt.%) was chosen to be a research object. Starting blanks

(disks with diameter 10 mm and 0.7 mm thick) were quenched at 920°C (30 min) and tempered at 670°C (1 hour). High-pressure torsion (HPT, P = 4 GPa) had been carried out for five complete revolutions at ambient temperature. After HPT samples had been annealed in helium atmosphere at 500°C with further water quench, annealing duration is 1 hour.

Samples structure had been studied by transmission electron microscopes (TEM) Technai G2 FEI and JEM 2100 at the accelerated voltage 200 kV. Middle part of the disks radius were taken to analyze samples microstructure after HPT. Disks ≈ 3 mm of diameter to be studied by electron microscope were made thinner up to ≈ 150 μm mechanically and further by electrolytic polishing at the device of Tinupol-5 in cooled electrolyte (95% of glacial acetic acid (CH_3COOH) + 5% of perchloric acid (H_3ClO_4)) to get appropriate thin sections to be analyzed. Average sizes of structure elements were determined by TEM dark-field images. Selected area electron diffraction (SAED) patterns indexing had been done by standard method described in details in [6]. Energy dispersive X-ray spectrometer INCA (EDS) was used to determine qualitative composition of dispersion particles. Samples microhardness had been measured by Vickers method on Duramin5 device at the loading 200 g. Average value of hardness had been calculated using measures on the middle part of disks radius.

X-ray research had been carried out with diffractometer Shimadzu XRD-6000 (with monochromator). Fine crystal structure parameters — microstrain of a crystal lattice and coherent scattering regions size — calculation is carried out by approximation method [7]. Dislocation density evaluation is carried out on the base of Bregg's maxima profiles analysis [8].

Equilibrium phase composition of steel in initial state and after annealing is calculated with a help of software Thermo-Calc (Thermo-Calc Software, Inc., McMurray, PA) and data base TCFE7.

3. Experimental results and discussion

Plastic deformation by high-pressure torsion resulted in formation of submicrocrystalline state with average size of structure elements of 100 nm and dispersed carbides (fig. 1 a, c) in steel Fe-Mo-V-Nb [9]. Structure has mixed character — dark-field analysis of images proves formation of microcrystallites with high-angle misorientations, subboundaries and high dislocation density (fig. 1 c).

Structure elements boundaries have diffuse contrast at TEM images (fig. 1 a, c). X-ray patterns analysis proves the formation of nonequilibrium polycrystalline structure after HPT: X-ray lines are broadened after deformation, microstrain of the crystal lattice is high ~10^{-3}, coherent scattering regions size, on the contrary, is low — 80 nm (table 1). After HPT in steel structure one could see globules of cementite type M_3C (15 – 20 nm) and ultrafine (< 5 нм) phases MC (M=V, Nb, Ti) and M3C [9]. Analysis of carbide subsystem after HPT is complicated by high dispersion and deformation of the main phase (ferrite). In initial state (before HPT), rather coarse spherical (90 nm) and small (15 – 20 nm) particles of cementite type and MC fine phase based on vanadium, titanium and niobium (6 – 7 nm) were seen in the structure under TEM researches. Fine phase was distributed in the structure in a quasi-homogeneous way, while coarse particles were located both on the boundaries and in the grains bodies [9]. Phase rating in steel Fe-Mo-V-Nb in equilibrium (before torsion) and after HPT allows to make an analysis of transformations in carbide subsystem at deformation. Deformation temperature is low (ambient) and even taking into account sample warming up during HPT, transformations in carbide subsystem are the results of plastic deformation first of all. High-pressure torsion helps initial cementite particles grinding (90 nm and 15 – 20 nm) down to 15 – 20 nm (can be seen seldom) and 3 – 4 nm. Ultrafine (nanoscale) phase MC (<5 нм) based on V, Nb, Ti is presented in the steel composition after high-pressure torsion. Dispersion phases MC and M_3C are distributed evenly in the structure and it's difficult to divide them.

After 1 hour annealing at 500°C crystallite size (according to TEM) is not changed in the steel subjected to HPT, and microhardness goes higher (6.4 HPa) compared to state after HPT (6.0 HPa). Annealing at 500°C of the steel doesn't cause the structure elements growth but resulted in its partial relaxation. It is proved by TEM images and X-ray structural analysis that X-ray lines turn thinner, crystal lattice microdestrain decreases, dislocations density goes down (Table 1). The structure as before is submicrocrystalline and nonequilibrium, structure elements boundaries are not clear often, subgrains and microcrystallites have a high density of dislocations (fig.1 b, d). The average size of microcrystallites after HPT and annealing at 500°C determined by dark-field TEM images amounts to 112±63 nm (fig. 1 d, f). Structure elements distribution according to size is close to the state after HPT (fig. 1 f). SAED patterns for these structures are of quasi-ring type, but if compare the state after HPT there are less azimuthal reflection diffusions on the rings (fig.1 e), i.e. large-angle misorientations prevail in the structure after annealing. After annealing at 500°C, grain — subgrain steel structure is stabilized by carbide phase. SAED patterns showed solid rings to prove small-size particles presence, dot reflections relevant to coarse carbides were found as well (fig. 1 e). Compared to the state after HPT the diffuse rings corresponding nanoscaled carbides have visible radial diffusion, interplanar spaces for such particles can be identified as corresponding to both MC and M_3C carbides. This fact allows one to assume that additional nano-scaled cementite particles are formed during annealing at 500°C due to decomposition of the carbon solid solution (due to decomposition and partial solution of cementite particles during HPT). Indexing of SAED patterns together with EDS analysis prove presence of small-size particles MC (M=Nb, V, Ti) evenly distributed in grain bodies. According to dark-field analysis of TEM-images their size is 3 – 4 nm. Equiaxed particles of cementite type M_3C (M=Fe, Cr) of 15 – 20 nm are found as well.

Data on carbides compositions determined on the base of electron diffraction analysis of steel structure after HPT and annealing and calculated (for equilibrium state at appropriate temperatures) with Thermo-Calc software are given in the Table 2.

Analysis of the Table 2 shows that the particles MC (<5 nm) based on vanadium, niobium and titanium which were seen in the steel structure both in initial state and after HPT and annealing at 500°C are stable phase for steel Fe-Mo-V-Nb irrespective of deformation and thermal treatment carried out in the present investigation. They provide steel dispersion harderning and determine thermal stability of the formed submicrocrystalline structure to annealing at the temperatures below the coagulation start one (higher than 700°C [10]).

High-pressure torsion results in grinding of cementite type particles, i.e. after deformation their contribution into hardening is increased, they also can be responsible for thermal stability of the structure but less than MC nano-scaled particles. Contribution of solid solution hardening into steel strength is negligible. After HPT, carbon concentration in solid solution can increase due to partial dissolution of the cementite type particles, but this increase is not considerable — according to X-ray structural analysis lattice parameter is changed within the experimental error.

Contribution of dispersion hardening in studied steel can be evaluated by equation of Orowan-Ashby [11]:

$$\sigma_{ps} = \left(\frac{0.538Gbf^{1/2}}{d}\right)\ln\left(\frac{d}{2b}\right),$$

where f is particles volume fraction; d is average particles diameter, G is a shear module (81.6 HPa), b is the Burgers vector (0.248 nm). According to the transmission electron microscopy data on carbides size and their volume fraction after high annealing temperatures (more than 500°C), when it is rather easy to determine the value of f, the fraction f = 0,03% for MC and f = 0,3% for cementite particles. It is easy to determine after annealing at 600°C when cementite type particles coagulate and cubic carbides based on heat-resistant elements are not changed.

If assume at first approximation that all cementite is dissolved at HPT and is precipitated as nano-scaled particles at the annealing at 500°C, at this size and distribution of the particles MC are not changed it could cause the hardening $\Delta\sigma_{ps}$=300 MPa (or $\Delta H\mu\approx$0.9 GPa). The softening due to decarburization of the matrix is small $\Delta\sigma_{ss}$<14 MPa ($\Delta H\mu$<40 MPa) even if assume that all carbon was in solid solution after HPT.

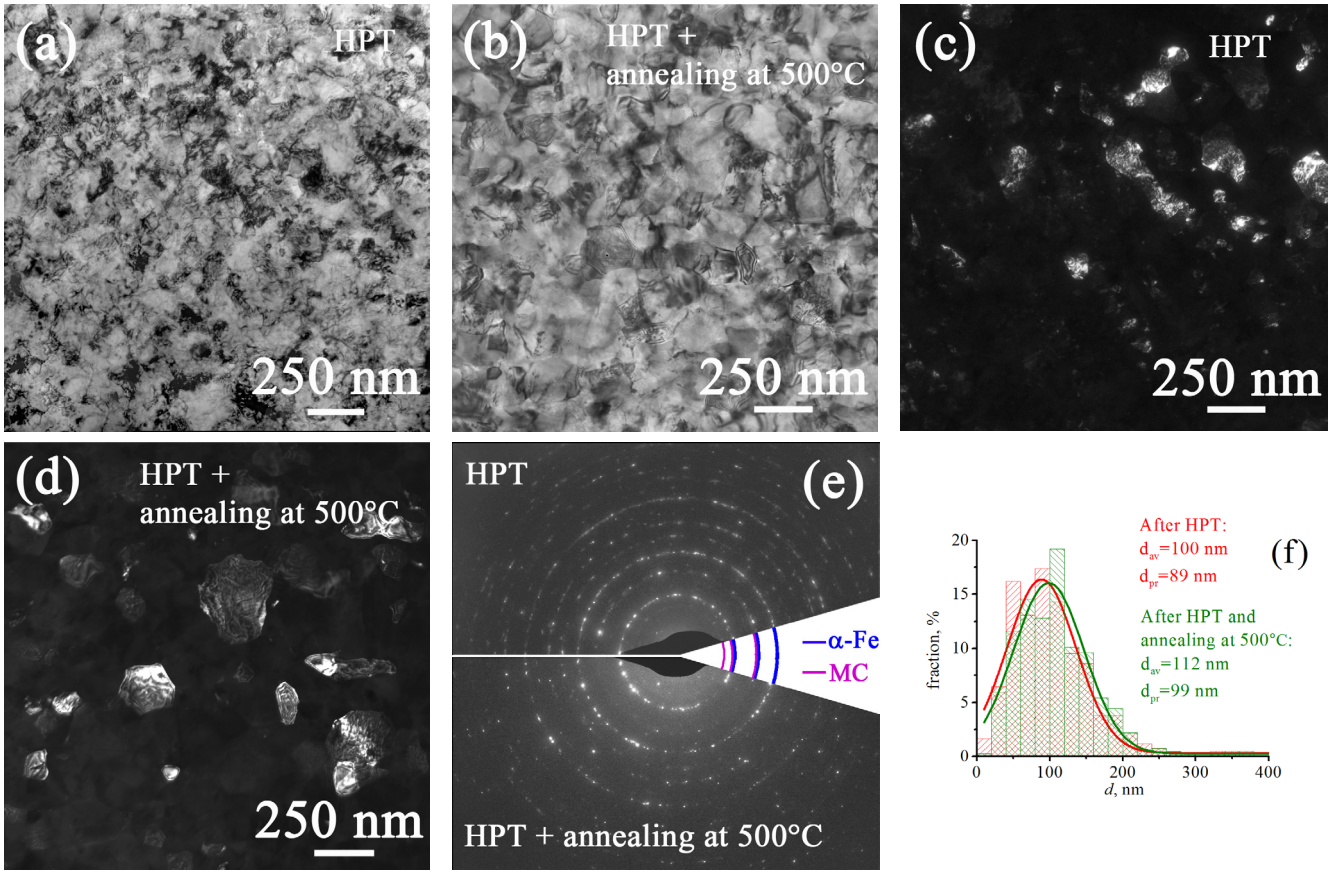

Fig. 1. Brigth-field (a, b) and dark-field (c, d) TEM images, SAED patterns (e) and distributions according to the sizes of the structural elements (f) for the steel after HPT (a, c, e, f) and subsequent annealing at 500°C (b, d, e, f). Dark-field images (c, d) were obtained in matrix reflections (011) α-Fe. SAED patterns (e) correspond to the areas of 0.95 μm^2.

Table 1. The effect of HPT and subsequent annealing at 500°C on a crystal lattice parameter a, sizes of a coherent scattering regions D_{hkl}, microstrain of the crystal lattice $\Delta d/d$, width of X-ray lines β and dislocation density ρ in the steel

State	a, nm	D_{hkl}, nm	$\Delta d/d$	$\beta_{(110)}/\beta_{(220)}$, degrees	ρ, cm^{-2}
HPT	0.2868	80	3.5×10^{-3}	0.318/0.814	6.0×10^{10}
HPT + annealing at 500°C	0.2866	70	1.2×10^{-3}	0.107/0.198	2.3×10^{10}

Changes of dislocation density at the annealing (500°C) also cause the microhardness decrease for $\Delta\sigma_\rho$=170 MPa (or $\Delta H\mu\approx$0.5 GPa) according to the well-known Orowan equation:

$$\Delta\sigma_\rho = \alpha MGb(\rho_{HPT}^{1/2} - \rho_{HPT+ann}^{1/2}),$$

where α=0,3; M=3.06 is a Talor factor; G=81.6 GPa is a shear module; b is the Burgers vector; ρ_{HPT} and $\rho_{HPT+ann}$ is dislocations densities after HPT and annealing respectively (table 1).

Thus, total growth of microhardness at dispersion hardening (assuming there are only nano-scaled particles) and softening due to decarburization and dislocations density decrease will amount to no more than 0,4 GPa which is close to observed microhardness difference for two studied states. The experimental data shows the presence of nano-scaled particles of cementite type together with coarser particles (15 nm) in the steel structure, the latter will contribute much less into hardening, i.e. it is not possible to explain microhardness growth of steel after HPT only by dispersion hardening.

Though the annealing at 500°C doesn't result in complete improvement of the steel structure after HPT, volume fraction of the high-angle boundaries increases evidently. At the heating of submicrocrystalline structure of mixed type primary recrystallization starts from separate grains growth, their nuclei are microcrystallites formed during deformation [3].

Analysis of TEM images of steel structure shows that these recrystallization nuclei are formed after HPT and annealing at 500°C. They have the equilibrium high-angle boundaries (with band contrast), don't contain dislocations and their sizes are similar to elements of grain-subgrain structure formed under HPT (figure 1 b, d). These nuclei neighbour with microcrystallites formed at HPT, which have high dislocation density even after annealing.

In other words, after HPT and annealing at 500°C more homogeneous submicrocrystalline structure with mainly high-angle misorientations between microcrystallites is formed in steel Fe-Mo-V-Nb. This works [3] shows that formation of thermally activated nuclei causes some increase of microhardness during recrystallization (at 450°C) in armco-iron subjected to high-pressure torsion. Therefore, increase of high-angle misorientations due to improvement of deformed structure and growth of thermally activated nuclei of recrystallization is the second factor to determine microhardness growth of steel at annealing within thermal stability interval.

4. Conclusions

Plastic deformation by high-pressure torsion resulted in formation of mixed submicrocrystalline structure (d = 100 nm) stabilized by dispersion carbides in steel Fe-Mo-V-Nb. After 1 hour annealing at the temperature 500°C, average size of structure elements (microcrystallites, d = 112 nm) and the character of their distribution according to size are changed insignificantly if compare with the state after HPT. Steel microhardness increases from 6.0 GPa in a state after high-

Table 2. Experimental (TEM, EDS) and calculated (using the Thermo-Calc software) data on the phase composition of steel after various treatment regimes (for calculated data — for different temperatures)

Treatment or temperature	Experimental data	Calculated using Thermo-Calc
T=920°C	—	***γ*-Fe** (Fe, Cr, Mn, Si, Ni, Cu, Mo, V, Al, Ti, Nb, C); **MC** (***Nb***, ***Ti***, ***V***, ***C***)
T=670°C	—	***α*-Fe** (Fe, Cr, Mn, Si, Ni, Cu, Mo, V, Ti, Nb, C); **M_3C** (***Fe***, ***Cr***, ***C***, Mn, V, Mo, Ni); **MC** (***V***, ***C***, Cr, Ti, Mo, Nb); **MC** (***Nb***, ***Ti***, ***Cr***, ***C***, V)
Quenching from 920°C + annealing at 670°C	***α*-Fe**; **M_3C** (Fe, Cr, Mn), d = 90 nm; **M_3C** (Fe, Cr, Mn), d = 15 – 20 nm; **MC** (V, Nb, Ti), d < 5 nm	—
HPT	***α*-Fe**; **M_3C** (Fe, Cr, Mn), d = 15 – 20 nm; **M_3C** (Fe, Cr, Mn), d < 5nm; **MC** (V, Nb, Ti), d < 5 nm	—
T=500°C	—	***α*-Fe** (Fe, Mn, Cr, Si, Ni, Cu, Mo, V, Ti, Nb, C); **FCC-phase** (Cu, Mn, Mo, Fe); **MC** (***V***, ***C***, Cr, Fe, Mo, Ti, Nb, Mn); **MC** (***Cr***, ***Nb***, ***Ti***, ***C***, Mn, Mo, Fe); **M_3C_2** (***Cr***, ***C***, V, Mo)
HPT + annealing at 500°C	***α*-Fe**; **M_3C** (Fe, Cr, Mn), d = 15 – 20 nm; **M_3C** (Fe, Cr, Mn), d < 5nm; **MC** (V, Nb, Ti), d < 5 nm	—

pressure torsion up to 6.4 GPa after HPT and annealing at 500°C.

Partial relaxation of structure and boundaries formed by severe plastic deformation takes place in steel after annealing as well as formation of thermally activated recrystallizing nuclei which size is close to one of crystallites and subgrains formed at torsion. Dispersion hardening — formation of nano-sized particles at annealing of deformed steel and increase of fraction of high-angle misorientations due to improvement of deformed structure and growth of thermally activated recrystallization nuclei provides keeping the high values for microhardness and submicrocrystalline structure of Fe-Mo-V-Nb steel after annealing at 500°C.

Acknowledgements. The work was partially supported by the program for basic research of Siberian Department of the Russian Academy of Science for 2013 – 2016 (III.23.2.2.) and RF President scholarship (SP-4682.2013.1). Equipment of Belgorod State National Research University and Novosibirsk State Technical University was provided to carry out this investigation.

References

1. N.I. Noskova, R.R. Mulyukov. Submicrocrystalline and nanocrystalline metals and alloys. Ekaterinburg, UrO RAN. (2003) 279 p. (in Russian) [Н.И. Носкова, Р.Р. Мулюков. Субмикрокристаллические и нанокристаллические металлы и сплавы. Екатеринбург, УрО РАН. 2003. 279 с.]
2. R.Z. Valiev, I.V. Alexandrov. Bulk nanostructured metallic materials. Moskow. IKZ «Akademkniga». 2007. 398 p. [Объемные наноструктурные металлические материалы: получение, структура, свойства. Москва. ИКЦ «Академкнига». 2007. 398 с.]
3. L.M. Voronova, M.V. Degtyarev, T.I. Chashchukhina. Fizika Metallov i Metallovedenie. **98**, 1 (2004). (in Russian) [Л.М. Воронова, М.В. Дегтярев, Т.И. Чащухина. Физика металлов и металловедение. **98**, 1 (2004)].
4. M. Papa Rao, V. Subramanya Sarma, S. Sankaran. Mater. Sci. Eng. A **568**, 171 – 175 (2013), doi:10.1016/j.msea.2012.12.084.
5. G.G. Maier, E.G. Astafurova, H.J. Maier, E.V. Naydenkin, G.I. Raab, P.D. Odessky, S.V. Dobatkin. Mater. Sci. Eng. A **581**, 104 – 107 (2013), doi:10.1016/j.msea.2013.05.075.
6. D.B. Williams, C.B. Carter. Transmission Electron Microscopy. Textbook for Materials Science. Springer, USA. (2009) 757 p.
7. S.S. Gorelic, Yu.A. Skakov, L.N. Rastorguev. X-ray diffraction and electron-optical analysis. Moscow, MISIS. (2002) 360 p. (in Russian) [С.С. Горелик, Ю.А. Расторгуев, Л.Н. Скаков. Рентгенографический и электронно-оптический анализ. Москва, МИСИС. 2002. 360 с.]
8. G.K. Williamson, R.E. Smallman. Phil. Mag. **1**, 34 – 46 (1956), doi:10.1080/14786435608238074.
9. G.G. Maier, E.G. Astafurova, V.S. Koshovkina, G.V. Chomyakova, E.V. Naydenkin, P.D. Odessky, S.V. Dobatkin. IOP Conf. Series: Mater. Sci. Eng A. **63**, 1, (2014) 012133, doi:10.1088/1757-899X/63/1/012133.
10. T. Gladman. Mater. Sci. Technol. **15**, 30 – 36 (1999).
11. H.K. D. H. Bhadeshia, R.W. K. Honeycombe. Steels. Microstructure and properties. Elsevier Ltd., Oxford, UK. 2006. 344 p.